Chlorpromazine toxicity is associated with disruption of cell membrane integrity and initiation of a pro-inflammatory response in the HepaRG hepatic cell line

Biomedicine & Pharmacotherapy 111 (2019) 1408–1416

Contents lists available at ScienceDirect

Biomedicine & Pharmacotherapy

journal homepage: www.elsevier.com/locate/biopha

Original article

Chlorpromazine toxicity is associated with disruption of cell membrane integrity and initiation of a pro-inflammatory response in the HepaRG hepatic cell line

Katie Morgan[a,*], Nicole Martucci[b], Ada Kozlowska[a], Wesam Gamal[c], Fillip Brzeszczynki[a], Philipp Treskes[a], Kay Samuel[d], Peter Hayes[a], Lenny Nelson[e], Pierre Bagnaninchi[f], Joanna Brzeszczynska[a], John Plevris[a]

[a] Hepatology Laboratory, University of Edinburgh, Royal Infirmary of Edinburgh, Edinburgh, United Kingdom
[b] The University of Pittsburgh, Department of Pathology, School of Medicine, United States
[c] School of Electronic Engineering and Computer Science, Bangor University, Dean Street, Bangor, Gwynedd, LL57 1UT, United Kingdom
[d] Scottish National Blood Transfusion Service, Advanced Therapeutics, The Jack Copland Centre, 52 Research Avenue North, Edinburgh, United Kingdom
[e] Institute for BioEngineering (IBioE), School of Engineering, The University of Edinburgh, The King's Buildings, Edinburgh, EH9 3JL, United Kingdom
[f] MRC Centre for Regenerative Medicine, 5 Little France Drive, Edinburgh, EH16 4UU, United Kingdom

ARTICLE INFO

Keywords:
Chlorpromazine
HepaRG
Cell membrane
Tight junctions
ECIS
Pro-inflammatory
Impedance sensing
Adaptive response

ABSTRACT

Chlorpromazine (CPZ) is a neuroleptic drug and prototype compound used to study intrahepatic cholestasis. The exact mechanisms of CPZ induced cholestasis remain unclear. Rat hepatocytes, or a sandwich culture of rat and human hepatocytes, have been the most commonly used models for studying CPZ toxicity *in vitro*. However, to better predict outcomes in pre-clinical trials where cholestasis may be an unwanted consequence, a human *in vitro* model, based on human HepaRG cells, capable of real-time, non-invasive and label free monitoring, alongside molecular investigations would be beneficial. To address this we used the human hepatic HepaRG cell line, and established concentrations of CPZ ranging from sub-toxic, 25 μM and 50 μM, to toxic 100 μM and compared them with untreated control. To assess the effect of this range of CPZ concentrations we employed electrical cell-substrate impedance sensing (ECIS) to measure viability and cell membrane interactions alongside traditional viability assays, immunocytostaining and qRT-PCR to assess genes of interest within adaptive and inflammatory pathways. Using these methods, we show a concentration dependant response to CPZ involving pro-inflammatory pathway, loss of tight junctions and membrane integrity, and an adaptive response mediated by Cytochrome P450 (CYP) enzyme activation and up-regulation of membrane phospholipid and xenobiotic transporters. In conclusion, structural changes within the membrane caused by sub-toxic and toxic concentrations of CPZ negatively impact the function of the cellular membrane. Damage to efflux transport proteins caused by CPZ induce cholestasis alongside downstream inflammation, which activates compensatory responses for cell survival.

Lay summary: Chlorpromazine is a drug used to treat patients with schizophrenia, which has a known association with liver damage. Here we show that it causes inflammation and alters the cell membranes in liver and bile duct cells similar to what is seen within a human population. The initiation of the inflammatory response and changes to cellular structure may provide insight into the damage and disease process and inform medical treatment.

1. Introduction

Chlorpromazine (CPZ) has long been used as an *in vitro* model of intrahepatic cholestasis (IHC), as there is evidence that it causes impaired biliary function, though the mechanisms behind this are not fully understood and side effects are usually idiosyncratic [1–5]. Cholestasis is a condition characterized by impaired ability of the bile ducts to secrete bile acids, bilirubin and cholesterol [6]. There is currently a

* Corresponding author at: Hepatology Laboratory, University of Edinburgh, Royal Infirmary of Edinburgh, Chancellor's Building, 49 Little France Crescent, Edinburgh, EH16 4SB, United Kingdom.
E-mail address: Katie.Morgan@ed.ac.uk (K. Morgan).

https://doi.org/10.1016/j.biopha.2019.01.020
Received 11 October 2018; Received in revised form 4 January 2019; Accepted 6 January 2019

need within the pharmaceutical industry to predict cholestasis *in vitro* before drugs are submitted for pre-clinical trials. Investigating the mechanisms behind CPZ toxicity may be informative for studies of other xenobiotics known to target the biliary system/cholangiocytes and aid in pre-clinical toxicity studies.

HepaRG cells are an intrinsic co-culture of hepatocyte and cholangiocyte-like cells. In comparison to other human hepatic cell lines, such as C3A and HepG2, the HepaRG cell line has been found to be more metabolically active, has an improved culture longevity and stability of 4–6 weeks in culture [7]. The major advantages of utilising this cell line is the ability to study, in one culture, the interaction of hepatocyte and cholangiocyte-like cells. This results in a culture of polar hepatocyte cords alongside cholangiocytes, and the formation of tight junctions between the cells within 8 days [8]. Tight junctions consist of a network of proteins that act as a barrier, maintaining cell membrane integrity and controlling exchange of molecules and ions across the membrane. Within hepatocytes, tight junctions are critical in maintaining cellular integrity, preserving polarity, and formation of bile canaliculi [8]

Cell based impedance assays are an emerging technology due to their high sensitivity and quantitative nature. Cells behave as insulating particles that alter impedance measurements when cultured on top of micro-electrodes. Therefore, an increase in impedance is a reflection of cellular growth kinetics. Electrical cell-substrate impedance sensing (ECIS) is a label-free, real-time monitoring technology where changes associated with cellular events are reflected in the measured impedance, which encompasses resistive and capacitive components. A major advantage of ECIS is its ability to decouple parameters of cell growth and cell-cell interaction, through mathematical modelling, into changes in membrane integrity, quality of basolateral adhesion and cell-cell tight junctions, all contributing to changes in impedance over time [9,10].

This quantification is possible due to the multi-frequency biosensor within the ECIS Zθ instrument developed by Applied Biophysics. At low frequencies (10^2–10^4Hz), the current is unable to pass through the cell membrane so the behaviour of the current is dependent on its ability to move through intercellular junctions. At this frequency, the measured resistance correlates biologically to the integrity of tight junctions and basolateral adhesion. Changes in these parameters can be directly correlated to changes in expression of zonular occludins 1 (ZO1). At higher frequencies (> 10,000 Hz), the current is able to pass through the cells. Capacitive measurements are preferred at these frequency ranges as they reflect the electrode cell coverage and reveal data on the integrity of the cell plasma membrane.

Previously, we have used ECIS technology to demonstrate disruption of HepaRG cell tight junctions with a model hepatotoxin acetaminophen (APAP) [8]. Here we applied this technique to a cholestatic compound CPZ, alongside traditional viability assays (PrestoBlue and Total ATP), immunocytostaining of cytoskeletal component F-actin and tight junction protein ZO1. Molecular investigations into apoptotic, oxidative stress and inflammatory pathways aid our understanding of the mechanism of toxicity and development of IHC.

2. Materials and methods

Several studies on the plasma concentrations of CPZ in humans were undertaken in the 1970s when the drug was still readily prescribed. Two groups, Curry et al., and Wiles et al., both describe variations in plasma levels between patients receiving the same dose of CPZ and cite these variations to differences in absorption and metabolism of the drug [11,12]. This seems in line with the idiosyncratic nature of this drug where patients can have the same plasma level of CPZ but one receives therapeutic results while the other does not. This can also be compared to toxicity where plasma levels between patients are consistent, but one patient may experience toxicity at therapeutic plasma levels and another may not. Acutetox: 'an in-vitro test strategy for predicting human acute toxicity' describe a series of 8 fatal cases where blood plasma concentration was between 3 and 35 mg/l [13]. This variance is again explained by difference in intestinal metabolism [14]

As such we use Antherieu's concentrations based on *in vitro* toxicity with an IC50 of 80 μM (50% of cells are viable) where 25 μM remains non-toxic, 50 μM is sub-toxic and 100 μM results in a toxic concentration. This *in vitro* range encompasses the variation of non-toxic – toxic concentrations described by Acutetox [13].

On day 8 of culture human HepaRG cells were treated with these concentrations of CPZ and analysis was undertaken using ECIS, viability assays, immunostaining and qRT-PCR.

2.1. Drug

CPZ was obtained from Sigma-Aldrich (Product no: C8138) and stored at room temperature. A stock of 100 mM in PBS buffer was aliquoted and stored at -20C. CPZ dilutions were made in HepaRG™ Maintenance and Metabolism Medium (ADD620).

2.2. Cell culture

HepaRG cells (HPR116 – cryopreserved HepaRG™ cells; Biopredic Int'l, Rennes, France) were cultured using suppliers' protocols. Williams E Medium with GlutaMAX™ was used as the basal medium with supplements purchased from Biopredic Int'l. Cells were seeded in General Purpose HepaRG® medium (ADD670) on day 0 at $2.4 \times 10^5/cm^2$into 8 well Ibidi arrays with 10+ electrodes per well for ECIS impedance measurements and on Corning 96 well and 24 well tissue culture plates for assays and immunocytochemistry respectively. On day 3 media was changed to HepaRG™ Maintenance and Metabolism Medium (ADD620) and renewed every other day. Cultures were monitored for 8 days before exposure to CPZ.

2.3. Immunocytostaining

The morphology of HepaRG cells cultured on 24 well plates was regularly assessed by microscopy before addition of 0, 25, 50 or 100μM CPZ on day 8 for 24 h. For immunocytostaining cells were fixed in 4% buffered formaldehyde solution (Pierce, 28908, Thermo Scientific) for 1 h, permeabilised with 0.1% Triton-X 100 (X100; Sigma-Aldrich) in Tris-buffered Saline (TBS; T6664; Sigma-Aldrich) for 30 min, and blocked with 5% goat serum (G6767; Sigma-Aldrich) in TBS for one hour. Tight junctions were stained using primary antibody to ZO1 (SC 10,804 Santa Cruz 1:50 dilution) incubation overnight and washed before addition of secondary antibody goat-anti-rabbit Alexa Fluor 488 (11,034; Life Technologies; 1:1000 dilution). Hoechst 33,342 (HS1492; Life Technologies; 10 μg/ml) and Phalloidin-TRITC (R415; Life Technologies; 3 U/mL 1:200 dilution) were used to stain nuclei and F-actin cytoskeleton respectively. Manufacturer's guidelines for Hoechst incubation suggest 5–30 minutes at room temperature as staining intensity may increase with time. Manufacturer's guidelines for Phalloidin suggest incubation from 30 to 60 minutes at room temperature. For ease of experimental design, Hoechst, Phalloidin and secondary antibody were added at the same time and were incubated for 2 h. While it is not necessary to incubate fixed cells with Hoechst or Phalloidin for this length of time, the nature of the chemical staining is such that no detrimental effect has been seen when incubating 2 h alongside secondary antibody. Fluorescent imaging was taken with an EVOS Auto FL imaging platform (Thermo Scientific) for cytoskeleton labelling. All images x20 magnification. Morphology of cultured cells was monitored throughout culture.

2.4. Viability assays

Cells were seeded on a 96 well standard tissue culture plate and cultured for 8 days. After 24-hour treatment with CPZ, supernatant was

removed and PrestoBlue® (A-13262; Life Technologies Paisley, UK) was added to each well and incubated for 30 min at room temperature. Fluorescence was measured using a GloMax + Microplate Multimode Reader (Promega, Southampton, UK) at 520 nm per vendor's instructions. After treatment with PrestoBlue assay wells were washed and cells lysed using Promega CellTiter-Glo®Luminescent Cell Viability Assay (G7570; Promega) luciferase based assay. After 30 min incubation at room temperature, detection agent was added and bioluminescent signals measured with the GloMax plate reader.

2.5. Molecular analysis

2.5.1. RNA isolation and reverse transcription-quantitative polymerase chain reaction (qRT-PCR)

RNA was extracted from untreated control and CPZ treated (25μM and 50μM) HepaRG cells. Total RNA was isolated using TRIzol™ (Thermo Fisher Scientific, Inc.), following the manufacturer's instructions. RNA was quantified using a Nanodrop instrument (ND 1000 Spectrophotometer). Quality and purity of RNA was examined using 260/280 and 260/230 absorbance ratios. All samples had 260/280 ratios above 1.8. The nanoScript to RT kit (PrimerDesign, UK) was used to convert 1 μg of RNA to cDNA following the manufacturer's instructions.

The quantitative validation of the expression of selected genes was assessed by RT-qPCR, as previously described [15] using custom PrimerDesign primers and applying the PrecisionPLUS qPCR Master Mix (PrimerDesign, UK), following the manufacturer's protocol. Primers are listed in Table 1. Amplification was performed for each cDNA (25 ng) sample in triplicate. Reactions were run in triplicate on a LightCycler Instrument (Roche LightCycler® 96 System). Running conditions were 95 °C 2 min, followed by 40 cycles of 95 °C 15 s and 60 °C 60 s. Data from qRT-PCR were normalized to multiple internal control genes (GAPDH, UBC, TOP1) with the geNorm algorithm as described by Vandesompele et al., 2002 [16,17].Results are presented as fold-changes in gene expression relative to untreated control calculated with the ΔΔCq method.

2.5.2. Identification of suitable reference genes

As previously described, the geNorm Housekeeping Gene Selection Kit (PrimerDesign) was used to evaluate expression of 12 commonly used housekeeping genes in untreated control and CPZ treated cells. Selected reference genes were: 18S (18S ribosomal RNA subunit), β-Actin(beta-actin), ATP5b (ATP synthase subunit 5b), B2M (beta-2microglobulin), TOP1 (topoisomerase 1), CYC1 (cyclin D1), EIF4a2 (eukaryotic initiation factor 4a2), GAPDH (glyceralde-hyde-3-phosphate dehydrogenase), RPL13a (ribosomal protein L13a), SDHA (succinate dehydrogenase complex, subunit A), UBC (ubiquitin C), and YHWAZ (phospholipaseA2). The geNorm output ranked the candidate reference gene according to their expression stability (M). The top three reference genes (GAPDH, UBC, TOP1) were used in subsequent analyses.

2.6. Electric cell-substrate impedance sensing (ECIS) – impedance assay

The ECIS Zθ system (Applied Biophysics) was used to measure, in real time, total impedance using a multiple frequency model. Using the ECIS-Zθ software's built-in mathematical model we were able to analyse the electrical current pathways which allows the data to be deconvolved into cell-cell tight junctions (Rb), cell-electrode basolateral adhesion (α) and cell membrane capacitance (Cm). HepaRG cells were seeded in 8 well 10+ electrode (8w10E+) cultureware (Ibidi). Differentiation of HepaRG cells into a stable and confluent co-culture of cholangiocyte-like cells and hepatocytes was monitored using phase microscopy alongside the ECIS–Zθ mode over 8 days (n = 3). A baseline for confluency before addition of compound, had already been established in our lab [8]. ECIS measurements were taken at 180 s intervals over a 500 Hz to 64 kHz frequency range. At day 8 HepaRG cells were challenged with a serial dilution of CPZ. Impedance measurements were normalized to the values at 0 h and modelled to a no cell control.

2.7. Statistical analyses

Data analysis and graphical illustration were performed with GraphPad Prism 5.0 and 7.0 (GraphPad Software, Inc., San Diego, CA, USA). Experiments were performed in triplicate, unless stated otherwise, and results are presented as mean ± SD. Differences between the different culture conditions (with or without CPZ) were detected applying a one way Anova with post hoc Tukey test. Results were considered significant at $p < 0.05$. Impedance data analysed using Matlab.

3. Results

3.1. Immunocytostaining

Cytoskeletal changes were assessed by staining with phalloidin at 24 h post CPZ treatment. Little difference was seen between control and 25μM CPZ treated cells. Using 50μM concentration, some degradation of F-actin cytoskeleton was evident. At 100μM, while there were still some nuclei present as evidenced by Hoechst nuclei staining (blue), there were few intact cells present and loss of phalloidin staining was evident.

The network of ZO1 staining pattern was not significantly different between control and 25 μm CPZ. Though it did appear that there was more intense staining, possibly compensatory at 25 μm. At 50μM ZO1 staining there was lack of organisation of hepatocyte chords as well as disruption to network of tight junction protein. At 100μM little to no cell/cell contact could be demonstrated by ZO1 staining (Fig. 1).

3.2. Total ATP and PrestoBlue assays

There was no statistical difference in cellular viability between control and CPZ treated samples at any concentration as evidenced by total ATP and PrestoBlue assays (n = 3) (Fig. 2).

Table 1
List of primers for genes of interest used within this study.

Gene	Forward Primer	Reverse Primer	Accession #
ABCB1	AACACCACTGGAGCATTGAC	TACAGCAAGCCTGGAACCTA	NM_000927
ABCB4	GAAGCAAAGAAACTCAATGTCCAG	TAGGCAATATTCTCGGCAATGC	NM_000443.3
ABCB11	CACAGACCAGGATGTTGACAGG	GTCTCAAGTGCTTCAATGAACCG	NM_003742.2
IL6	GCAGAAAACAACCTGAACCTT	ACCTCAAACTCCAAAAGACCA	NM_000600
BAX	ATGGAGCTGCAGAGGATGAT	CAGTTGAAGTTGCCGTCAGA	NM_138761
BCL2	GAGGTCACGGGGGCTAATT	GAGGCTGGGCACATTTACTG	NM_000633
TNF	AGGTTCTCTTCCTCTCACATAC	ATCATGCTTTCAGTGCTCATG	NM_000594
HNF	GACCTCTACTGCCTTGGACAA	GATGAAGTCGGGGGTTGGA	NM_000457
NRF2	CCCAGCACATCCAGTCAGA	CAGTCATCAAAGTACAAAGCATCT	NM_006164
CYP3 A4	ACCGTAAGTGGAGCCTGAAT	AAGTAATTTGAGGTCTCTGGTGTT	NM_017460

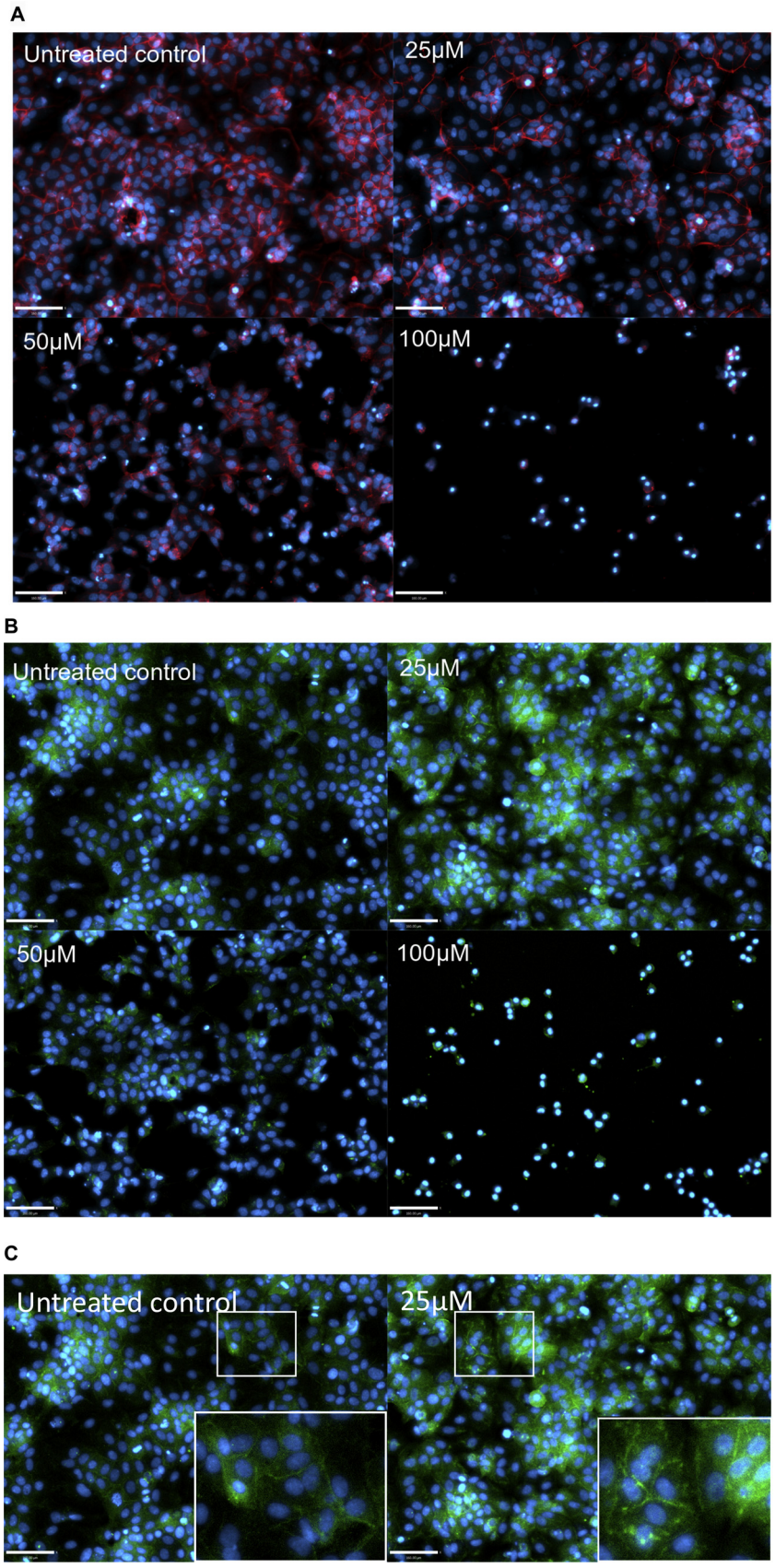

Fig. 1. Immunocytostaining of HepaRG cells after 24 h exposure to increasing concentrations of CPZ: (**A** HepaRG cells double stained on day 8 with Hoechst (blue nuclei stain) and Phalloidin (red F-actin cytoskeletal stain) reveals distinct pericanalicular-cytoskeletal/ TJ-associated F-actin bands in control cells with decreased staining at low-dose (25 μM) CPZ and progressively less intense staining at higher CPZ doses. (**B**) Double staining of HepaRG cells on day 8 with Hoechst (blue nuclei stain) and ZO1 (green staining indicating tight junction protein) demonstrated reduced intensity of the hepatic tight junction-associated structural protein ZO1. ZO1, progressively decreases, as the hepatic cord phenotype is compromised at 50 and 100 μM concentrations. (**C**) Untreated control and 25 μM CPZ shown with magnified field showing membrane bound ZO1 (For interpretation of the references to colour in this figure legend, the reader is referred to the web version of this article).
Scale bars represent 160 nm, all pictures taken on EVOS fl-auto at x20 magnification. Figures representative of 3 independent experiments with 3 technical replicates per experiment.

Viability assays were not in agreement with immunocytostaining at 100 μm. This indicated good viability of un-adhered cells within culture. This discrepancy can be explained by possible disruption of adhesion through wash steps, fixation and permeabilisation of the immunocytostaining that did not affect viability within the experiment period.

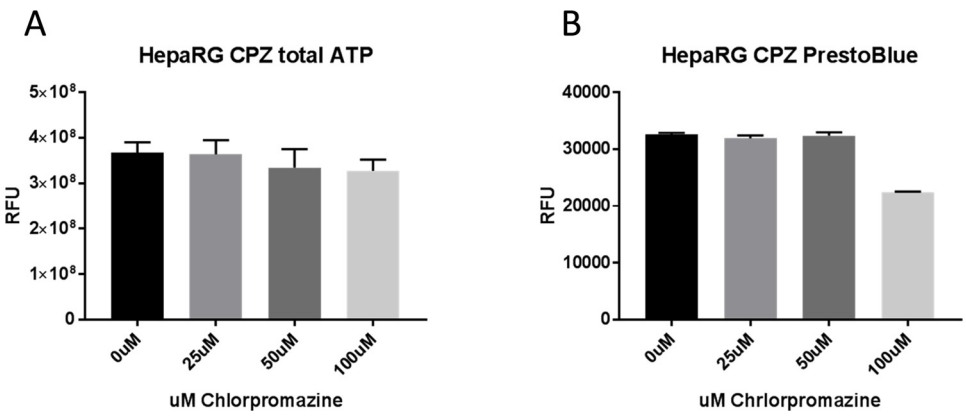

Fig. 2. Measurement of Cell Viability after 24 h incubation with increasing concentrations of CPZ: Cell viability of HepaRG cells were assessed using A) Promega total ATP assay and B) PrestoBlue resazurin based assay. Quantification of metabolic proficiency after 24 h exposure to various concentrations of CPZ shows no significant loss of viability at any concentration (Data indicative of 3 independent experiments with 3 technical replicates each experiment).

3.3. Effects of CPZ on tight junctions and basolateral adhesion

Total impedance (Z) is a composite value of resistive and capacitive parts, which can be further deconvolved into parameters that can measure biological behaviour.

Multiple frequency measurements using ECIS Zθ allowed modelling of the following parameters corresponding to biologically significant cell behaviour; Tight junctions (Rb), cell-electrode basolateral adherence (α), and cell membrane integrity (Cm).

The resistance showed a highly-sensitive concentration-response to CPZ with a decrease of impedance at all frequencies (Fig. 3A). The lowest concentration, 25μM, had least effect across all parameters.At 50μM both Rb and Cm decreased, however, after 5 h some recovery was seen (Fig. 3 B&D). 100μM CPZ showed the greatest loss of Cm with a decrease of approximately 50% within the first 2 h of administration, but also showed recovery 6 h post administration which continued throughout the duration of the experiment (Fig. 3D). Basolateral adhesion was the least effected parameter though some dose dependant response was seen (Fig. 3C).

Taken together deconvolved and resistance measurements were informative as to the mechanistic effect of CPZ revealing that tight junctions had been disrupted at 50 and 100μM concentrations while there was little effect on basolateral adherence. Overall membrane capacitance was most effected at 100μM concentration, but also showed some recovery in impedance at subtoxic (50 μM) and high concentration (100 μM) measurements (Fig. 3).

3.4. Expression of functional markers

Hepatocyte nuclear factor 4α (HNF4α) directly regulates expression of CYP3 A4, a major metabolic enzyme within the liver [18]. While HNF4α did not show a statistically significant increase at either 25 or 50μM, its up regulation at 25μM and low expression at 50μM correlated with the pattern seen in CYP3 A4 where expression was significantly up regulated at low concentration (25μM) CPZ ($p < 0.05$) when compared with untreated control. However, at 50μM CPZ, CYP3 A4 expression was down regulated when compared with 25μM ($p < 0.05$) (Fig. 4).

3.5. Anti-apoptotic pathway

Viability was unaffected with no initiation of apoptotic pathways as can be seen by the ratio of apoptotic and anti-apoptotic markers BAX and BCL-2 between 25 and 50 μM concentrations of CPZ ($p < 0.0001$). This was further supported by a progressive and significant induction of Bcl-2, from control to 50 μM CPZ treated cells (Fig. 6).

3.6. Changes in expression of biliary transporters

Expression of efflux phospholipid transporter ABCB4 showed a concentration dependant increase in response to CPZ, which was significantly different from control at 50μM ($p < 0.001$). ABCB1 responsible for xenobiotic efflux, was non-significantly down regulated at 25μM when compared to control. At 50μM ABCB1 was significantly up regulated as compared to 25μM CPZ, though not significantly different from control. Whereas, bile acid export pump ABCB11 was not detected at 25μM and was significantly down regulated at 50μM compared to control ($p < 0.01$) (Fig. 7).

When compared with untreated control, CPZ treated cells showed a statistically significant concentration dependant response in expression of pro-inflammatory cytokines IL-6 and TNF-α. Up regulation of IL-6 at 50 μM was almost a 10 fold increase compared to untreated control ($p < 0.005$) while TNFα showed a 2 fold increase at 25 μM ($p < 0.001$) and a 9 fold increase at 50 μM ($p < 0.005$) when compared to untreated control (Fig. 5).

The gradual increase in expression of anti-oxidant regulator NRF2, with increasing concentrations of CPZ, though not statistically significant is suggestive of cellular activation of this defence pathway, which is associated with CPZ induced cholestasis (Fig. 5).

4. Discussion

The HepaRG™ co-culture provides a unique opportunity to study the interaction of hepatocytes and cholangiocytes when challenged with CPZ.

Here we show, a novel approach to developing a mechanistic understanding of CPZ toxicity combining cell viability assays, impedance based quantitative measurements of cell membrane changes and gene expression data.

CPZ is a neuroleptic drug used in the treatment of schizophrenia that has been known to cause acute IHC. Current models fail to fully-explain the mechanism of CPZ toxicity, whether because of interspecies variation using animal derived hepatocytes or poor *in vitro* metabolic functionality found in human hepatic cell lines.

Tavoloni and Boyer describe the toxic effects of specific CPZ metabolites and how they affect bile secretion in rats leading to IHC [19]. They propose that any induction of the pathways involved in the metabolism of these toxic molecules could account for the idiosyncratic presentation. While their study highlights the many and varied metabolites of CPZ and how they interact with the cell membrane altering bile acid secretion, there is still an issue of interspecies variation. For example, bile acids vary in quality and quantity between animal and human counterparts and therefore results cannot be directly correlated [19]. Other studies using CPZ attribute incidence of IHC and cellular damage to increased inflammatory response [20]. However, many of these studies pre-treated cells to induce inflammation before use [21].

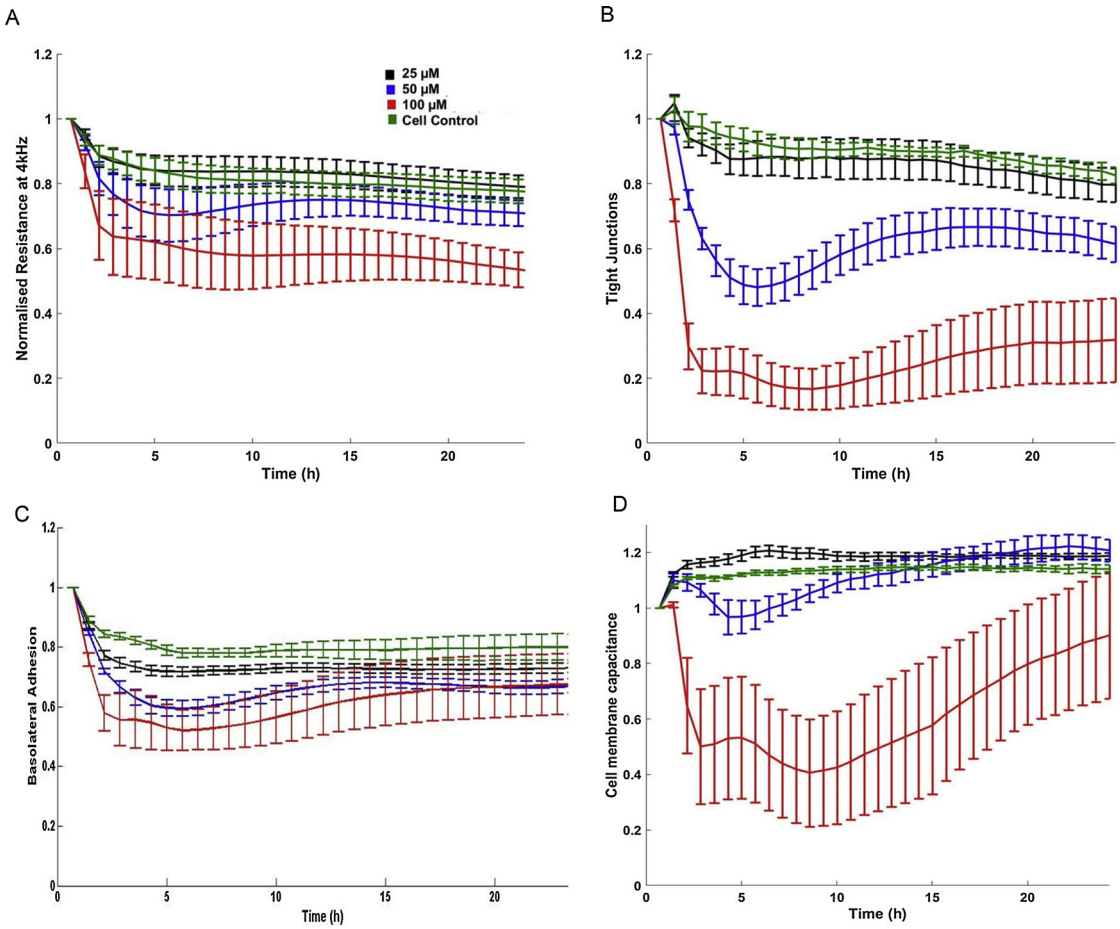

Fig. 3. Real time impedance measurements using ECIS Zθ system A) Post-challenge impedance kinetics showing 24hours treatment with CPZ in confluent HepaRG cells: CPZ caused a dose-dependent decline in normalized resistance - a global indicator of cellular status. B) **Rb (cell-cell tight junctions):** CPZ disrupted tight junctions in a concentration- and time- dependent manner; compared with control values. Subjecting HepaRG to 100µM CPZ caused Rb to decrease after 6 h with marginal recovery around 15 h. C) α **basolateral adhesion)**: Cell-substrate adhesion disruption was detected in a concentration dependent manner, suggesting some loosening of cells from the electrode surface. At 100µM CPZ, cell adhesiveness decreased, but showed an increase around 10 h suggesting re-adherence of cells. D) **Cm (membrane capacitance):** membrane capacitance, reflecting cell membrane integrity, was significantly compromised at 100µM CPZ beginning at 2 h post treatment. Some increase in Cm of 100µM CPZ was seen around 10 h which is consistent with the basolateral adhesion (α) and further indicating some cellular compensatory effect.

A fully functional *in vitro* human model would address issues of interspecies variation and would not need induction. Primary human hepatocytes are difficult to obtain and culture and can introduce variability due to intra-species variation, and many immortalised cell lines do not retain metabolic proficiency, which would preclude them for needing pre-conditioning. Therefore, we use the human HepaRG cell line which differs from traditional hepatic *in vitro* models, as it is propagated from a bipotent hepatoblast-like cell and differentiated with dimethylsulfoxide to a co culture of hepatocyte and cholangiocyte-like cells. These maintain intrinsically high CYP activity, and functionality

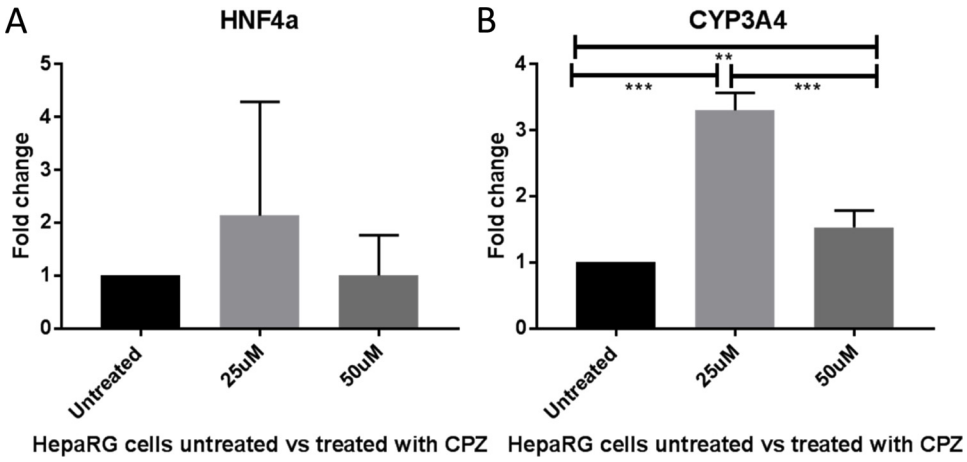

Fig. 4. Effects of CPZ on mRNA expression of HNF4α and CYP3A4: mRNA expression of **(A** nuclear factor HNF4α and **(B** CYP3 A4 in the HepaRG cells comparing untreated control, 25 µM and 50 µM CPZ. Fold change is relative to untreated control. Results show concentration dependent downregulation of mRNA levels of CYP3 A4 and HNF4α in 50µM CPZ treated cells compared with untreated control. Expression of CYP3 A4 was significantly upregulated at 25µM of CPZ ($p < 0.05$) when compared with untreated control which may be indicative of a compensatory response by the cell before significant downregulation at 50 µM. Fold change (± SD), data taken from three independent experiments using three technical replicates per experiment.

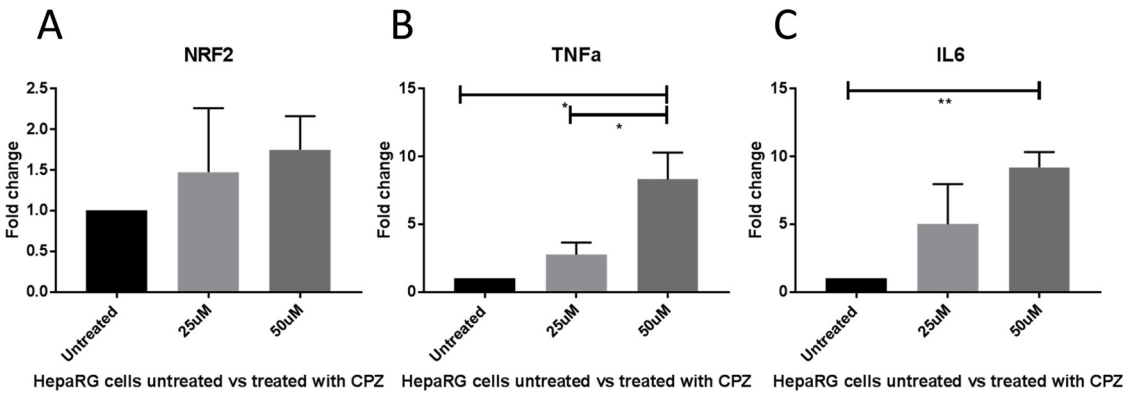

Fig. 5. Expression of cellular defence system and pro-inflammatory markers.
Expression of the oxidative defence and pro-inflammatory genes NRF2, TNFα and IL6 show a trend of upregulation at 25 and 50 μM treatment with CPZ compared to control with significant upregulation at 50 μM in both IL6 and TNFα
A) The mRNA expression of the oxidative defence gene NRF2 is increased in 50 μM treated cells when compared to untreated control. Though no significant difference is reported this trend is in line with both TNFα and IL6. Data taken from four independent experiments with three technical replicates per experiment **B)** Results show significant upregulation of mRNA expression of TNFα between 25 μM and 50 μM treated cells ($p < 0.001$) compared to untreated control. **C)** Expression of IL6 shows concentration dependent increasing trend when compared with untreated control, showing significance at 50μM ($p < 0.005$). Data taken from three individual experiments with three technical replicates per experiment.

akin to freshly isolated primary human hepatocytes. They also remain stable for several weeks, offering the opportunity to assess membrane transport proteins in a differentiated co-culture model known to metabolise both phase I and II enzymes [6]. Other studies of CPZ induced toxicity which used the HepaRG cells have attributed incidence of IHC to increased inflammatory response leading to oxidative stress and mitochondrial toxicity, which damages tight junctions and contributes to a more fluid cellular membrane [1]. Within our model we also show evidence of membrane changes *via* a concentration dependant inflammatory response most likely due to oxidative stress. However, this may represent an adaptive or compensatory response as suggested by partial recovery of impedance-based parameters with regards to overall cell membrane integrity.

There are many elements to the tight junction complex consisting of adherens, claudin and occludin proteins. ZO1 is attached to both claudin and occludin proteins and is anchored to the F-actin cytoskeleton. For this reason, we performed parallel staining of the F-actin cytoskeleton and membrane protein ZO1 which shows a loss of F-actin and ZO1 in a concentration dependent response to CPZ (Fig. 1).

Viability assays (PrestoBlue and ATP) showed no differences in viability between control and CPZ treated cells at the concentrations tested (Fig. 2). This appeared to contradict immunocytochemistry images where Hoechst staining for nuclei showed very few cells remained attached at 100μM CPZ 24 h post-treatment. We speculate non, or loosely, adherent cells which remained viable, would have been washed away during processing for staining, as these wash steps tend to be more aggressive than those between viability assays. [22] A measure of cell viability can also be seen when considering the ECIS data. At 24 h post treatment there is evidence that cells are still covering electrodes at the 50 and 100 μM concentrations. Although membrane integrity is compromised, it is possible that the cells which remain are still metabolically active. As the PrestoBlue assay measures the cells metabolic proficiency, it could be that at 100 μM, though there are fewer cells, metabolic activity may still be present.

While it has been well documented that CPZ causes cholestasis within a relatively short time frame [23] there are no *in vitro* studies to confirm or quantify how quickly the toxic effects of CPZ take effect. A real-time, label free method showing immediate cause and effect of drug toxicity would give more insight into pathophysiology.

Deconvolving impedance data showed a concentration dependent loss of tight junctions, and significant loss of membrane integrity at 100μM concentration within 6 h of CPZ treatment.

Some recovery of membrane integrity was seen after 6 h at 50 and 100μM. (Fig. 3). This result differs from our previously published ECIS monitoring of APAP which was used as a model hepatotoxin and showed concentration dependant damage to tight junctions with no recovery[8]. Signatures of dose dependant toxicity have also been demonstrated using other cell lines and treatments for example skin and retinal cells exposed to various wavelengths of light [24–26],. As ECIS is a highly sensitive technology, it is possible that different signatures could be seen depending on the mechanism of toxicity and further work with cholestatic compounds may establish an ECIS specific signature.

Metabolic activity and CYP functionality are important in detoxification of the cellular environment and support adaptive processes within the cell. Here both CYP3A4 and its regulator HNF4α showed a trend of up-regulation at the lower concentration indicating a possible adaptive response to low levels of toxicity within the cellular environment. (Fig. 4) The inhibition of CYP3A4 and HNF4α at the higher concentration of 50 μM may correlate with the up-regulation seen in IL6 and TNFα (Fig. 5), inducers of oxidative stress, which are known to cause down-regulation of these markers [20].

Expression of IL6 seen in instances of cellular stress and disease, is also known to induce the anti-apoptotic BCL2 pathway, shown in Fig. 6 and may also be indicative of a compensatory response [27]. A concentration dependant non-significant increase of NRF2, which regulates expression of antioxidant proteins, was also seen in response to CPZ and further suggests counteraction to toxicity.

In this study, we have not measured levels of TNFα and IL6 in media, instead we have looked at mRNA expression for these cytokines. We have shown that they are significantly different from control which indicates that changes in mRNA expression are due to CPZ treatment.

Inhibition of the bile acid transporter ABCB11 in the HepaRG model may point towards an additional mechanism of CPZ mediated cholestasis. Accumulation of bile acids has been shown to target the tight junction complex and more specifically ZO1 protein [28]. This may be the causative factor in the degradation of tight junctions and fluctuation of membrane integrity.

We also assessed xenobiotic and phospholipid transporters ABCB1 and ABCB4 and show a concentration dependant up-regulation of both genes which was significantly increased at 50 μM, indicative of an adaptive response at the cellular level. (Fig. 7). Polymorphisms of ABCB1 and ABCB4 have been associated with various forms of cholestasis and may go some way to addressing the idiosyncratic presentation of cholestasis caused by CPZ within a given population [29–32]. Within this model, these genes are up-regulated in response to sub toxic CPZ concentrations. We speculate that the inability to

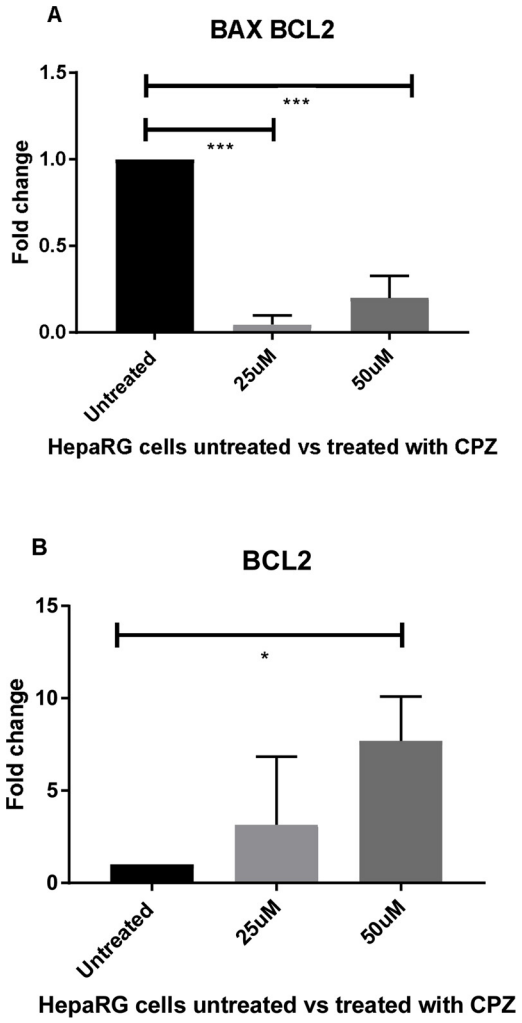

Fig. 6. Assessment of apoptotic and anti-apoptotic markers in HepaRG cells treated with CPZ: **A)** Statistically significant difference was seen in the BAX/BCL2 ratio indicating down regulation of apoptotic factors ($p < 0.0001$). **B)** This is supported by upregulation of anti-apoptotic marker BCL2 which shows significant increase to control ($p < 0.04$). Fold change in mRNA expression (± SD), data from three independent experiments with three technical replicates each experiment.

upregulate these transporters due to polymorphism or mutation may result in CPZ induced IHC and could explain why certain individuals are more susceptible than others.

5. Conclusion

Here we present a novel approach to forming a mechanistic view of CPZ toxicity

encompassing traditional cell viability assays, impedance based quantitative measurements and molecular investigation. CPZ treated HepaRG were viable and retained membrane integrity however, basolateral adherence and tight junctions were reversibly compromised. Gene expression analysis showed evidence of an adaptive response to CPZ treatment. Oxidative stress caused by inflammatory cytokines TNFα and IL6, known to down-regulate CYP3A4 activity, may have also contributed to the trend for increased NRF2 expression. In this model bile acid transporter ABCB11 was down regulated, this causes accumulation of bile acids leading to loss of tight junctions. Further evidence of an adaptive response lies in the up regulation of anti-apoptotic gene BCL2, xenobiotic and phospholipid transporters ABCB1 and ABCB4 also support an adaptive response to CPZ treatment. We speculate that the idiosyncratic presentation of CPZ induced IHC may be due to polymorphisms in ABCB1 and ABCB4 transporters, as some individuals are therefore unable to up regulate membrane bound transporters resulting in continued hepatic injury.

Authors contributions

Katie Morgan: Experiments, Design, Analysis and Writing of article
Nicole Martucci: Experiments within laboratory of University of Edinburgh
Kozlowska, Ada: Experiments
Gamal, Wesam: Concept, Experimental design and Expertise
Brzeszczynki, Fillip: Experiments and Analysis
Treskes, Philipp: Design
Samuel, Kay: Experimental Analysis, writing, proof reading
Hayes, Peter: Design, Proof reading
Nelson, Lenny: Concept and Design
Bagnaninchi, Pierre: Concept, Design, Expertise, Proofreading
Brzeszczynska, Joanna: Design, Experiments, Analysis, Writing
Plevris, John: Design, Analysis, Proofreading

Funding

The research carried out within this study was funded by The

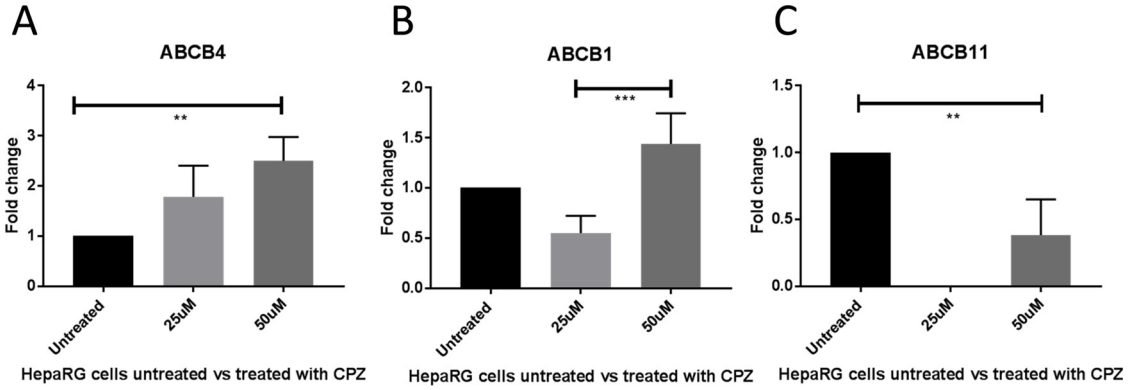

Fig. 7. Changes in membrane transport of HepaRG cells treated with increasing concentrations of CPZ: **A&B)** There was a concentration dependent increase of membrane bound drug efflux transporter ABCB4 ($p < 0.01$). and phospholipid transporter ABCB1 ($p < 0.001$) This increase was significant between untreated control and 50μM for ABCB4 and between 25μM and 50μM for ABCB1. **C)** Expression of bile acid transporter marker ABCB11 was not detected at low concentration CPZ and significantly down regulated at 50μM ($p < 0.01$). Fold change (± SD), data taken from four independent experiments with three technical replicates per experiment.

Hepatology Laboratory was supported by the Chief Scientist Office of Scotland (ETM/182) and the BBSRC (BB/L023687/1) during the period of this research.

Conflicts of interest

We the authors declare that there are no competing interests

References

[1] S. Antherieu, P. Bachour-El Azzi, J. Dumont, Z. Abdel-Razzak, C. Guguen-Guillouzo, B. Fromenty, M.A. Robin, A. Guillouzo, Oxidative stress plays a major role in chlorpromazine-induced cholestasis in human HepaRG cells, Hepatology 57 (4) (2013) 1518–1529.

[2] T. Akerboom, I. Schneider, S. vom Dahl, H. Sies, Cholestasis and changes of portal pressure caused by chlorpromazine in the perfused rat liver, Hepatology 13 (1991) 216–221, https://doi.org/10.1002/hep.1840130204.

[3] H.J. Zimmerman, J.H. Lewis, Drug-induced cholestasis, Med. Toxicol. 2 (2) (1987) 112–160.

[4] D. Moradpour, J. Altorfer, R. Flury, P. Greminger, M. Schmid, et al., Chlorpromazine-induced vanishing bile duct syndrome leading to biliary cirrhosis, Hepatology 20 (1994) 1437–1441, https://doi.org/10.1002/hep.1840200610.

[5] J.V. Castell, Maria J. Gomez-Lechon, X. Ponsoda, R. Bort, *In vitro* investigation of the molecular mechanisms of hepatotoxicity, *In vitro* Methods in Pharmaceutical Research, (1996), pp. 375–410 Chapter 16.

[6] S. Antherieu, C. Chesne, R. Li, C. Guguen-Guillouzo, A. Guillouzo, Optimization of the HepaRG cell model for drug metabolism and toxicity studies, Toxicol. Vitr. 26 (8) (2012) 1278–1285.

[7] L.J. Nelson, K. Morgan, P. Treskes, K. Samuel, C.J. Henderson, C. Lebled, N. Homer, H.M. Grant, P. Hayes, J. Plevris, Human hepatic HepaRG cells maintain and organotypic phenotype with high intrinsic CYP450 activity/metabolism and significantly outperform standard HepG2/C3A cells for pharmaceutical and therapeutic applications, Basic Clin. Pharmacol. Toxicol. 120 (1) (2017) 30–37.

[8] W. Gamal, P. Treskes, K. Samuel, G. Sullivan, R. Siller, V. Srsen, K. Morgan, A. Bryans, A. Kozlowska, A. Koulovasilopoulos, I. Underwood, S. Smith, J. Del-Pozo, S. Moss, A.I. Thompson, N.C. Henderson, P.C. Hayes, J. Plevris, P. Bagnaninchi, L. Nelson, Low-dose acetaminophen induces early disruption of cell-cell tight junctions in human hepatic cells and mouse liver, Sci. Rep. 7 (2017) 37541.

[9] J. Wegener, C.R. Keese, I. Giaever, Electric cell-substrate impedance sensing (ECIS) as a noninvasive means to monitor the kinetics of cell spreading to artificial surfaces, Exp. Cell Res. 259 (2000) 158–166.

[10] I. Giaever, C.R. Keese, Micromotion of mammalian cells measured electrically, Natl. acad Sci 88 (1991) 7896–7900.

[11] D. Wiles, T. Kolakowska, A. McNeilly, B. Mandelbrote, M. Gelder, Clinical significance of plasma chlorpromazine levels I. Plasma levels of the drug, some of its metabolites and prolactin during acute treatment, Psychol. Med. 6 (3) (1976) 407–415.

[12] S. Curry, J. Marshall, J. Davis, D. Janowsky, Chlorpromazine plasma levels and effects, Arch. Gen. Psychiatry 22 (4) (1970) 289–296.

[13] ACUTETOX, ACuteTox-Research Project for Alternative Testing, [online] EU contract no. LSHB-CT-2004-512051viewed 28/11/18 University of Oulu, Finland, 2004http://www.acutetox.eu/pdf_human_short/89Chlorpromazine%20hydrochloride%20revised.pdf.

[14] R.C. Baselt, R.H. Cravey, Disposition of Toxic Drugs and Chemicals in Man, 4th ed., Chemical Toxicology Institute, Foster City, California, 1995, pp. 158–162.

[15] F. Meier, N. Freyer, J. Brzeszczynska, F. Knospel, L. Armstrong, M. Lako, K. Zeilinger, et al., Hepatic differentiation of human iPSCs in different 3D models: a comparative study, Int. J. Mol. Med. 40 (6) (2017) 1759.

[16] J. Vandesompele, K. De Preter, F. Pattyn, B. Poppe, N. Van Roy, A. De Paepe, F. Speleman, Accurate normalization of real-time quantitative RT-PCR data by geometric averaging of multiple internal control genes, Genome Biol. 3 (2002) RESEARCH0034.

[17] J. Vandesompele, M. Kubista, M. Pfaffl, Reference Gene Validation Software for Improved Normalization, Real-time PCR: Current Technology and Applications, Caister Academic Press, 2009 ISBN:978-1-904455-39-4.

[18] H. Lu, Crosstalk of HNF4α with extracellular and intracellular signaling pathways in the regulation of hepatic metabolism of drugs and lipids, Acta Pharm. Sin. B 6 (5) (2016) 393–408.

[19] N. Tavoloni, J.L. Boyer, Relationship between hepatic metabolism of chlorpromazine and cholestatic effects in the isolated perfused rat liver, J. Pharmacol. Exp. Ther. 214 (2) (1980) 269–274.

[20] S. Chatterjee, L. Richert, P. Ausustijns, P. Annaert, Hepatocyte-based in vitro model for assessment of drug-induced cholestasis, Toxicol. Appl. Pharmacol. 274 (2014) 124–136.

[21] P. Bachour El-Azzi, A. Sharanek, A. Burban, R. Li, R. le Guevel, Z. Abdel-Razzak, B. Stieger, C. Guguen-Gouillozo, A. Gouillozo, Comparative localization and functional activity of the main hepatobiliary transporters in HepaRG cells and primary human hepatocytes, Toxicol. Sci. 145 (1) (2015) 157–168.

[22] D. Bhattacharyya, A.T. Hammond, B.S. Glick, High-quality immunofluorescence of cultured cells, Methods Mol. Biol. 619 (2010) 403–410.

[23] S. Zelman, Liver cell necrosis in chlorpromazine jaundice (allergic cholangiolitis): a serial study of twenty-six needle biopsy specimens in nine patients, Am. J. Med. 27 (5) (1959) 708–729.

[24] D. Bennet, B. Viswanath, S. Kim, J. An, An ultra-sensitive biophysical risk assessment of light effect on skin cells, Oncotarget 8 (29) (2017) 47861–47875.

[25] D. Bennet, S. Kim, Evaluation of UV radiation-induced toxicity and biophysical changes in various skin cells with photo-shielding molecules, Analyst 140 (18) (2015) 6343–6353.

[26] Devasier Bennet, Sanghyo Kim, Impedance-based cell culture platform to assess light-induced stress changes with antagonist drugs using retinal cells.(Author abstract), Anal. Chem. 85 (10) (2013) 4902–4911.

[27] A.B. Waxman, N. Kolliputi, IL-6 protects against hyperoxia-induced mitochondrial damage via Bcl-2-induced Bak interactions with mitofusins, Am. J. Respir. Cell Mol. Biol. 41 (4) (2009) 385–396.

[28] X. Chen, T. Oshima, T. Tomita, H. Fukui, J. Watari, T. Matsumoto, H. Miwa, Acidic bile salts modulate the squamous epithelial barrier function by modulating tight junction proteins, Am. J. Physiol. Gastrointest. Liver Physiol. 301 (2) (2001).

[29] H.E. Wasmuth, A. Glantz, H. Keppeler, E. Simon, C. Bartz, W. Rath, L.A. Mattsson, H.U. Marschall, F. Lammer, Intrahepatic cholestasis of pregnancy: the severe form is associated with common variants of the hepatobiliary phospholipid transporter ABCB4 gene, Gut 56 (2) (2007) 265–270.

[30] Eric Pasmant, Philippe Goussard, Laetitia Baranes, Ingrid Laurendeau, Samuel Quentin, Philippe Ponsot, B.éatrice Parfait, First description of ABCB4 gene deletions in familial low phospholipid-associated cholelithiasis and oral contraceptives-induced cholestasis, Eur. J. Hum. Genet. 20 (3) (2011) 277–282.

[31] Tougeron, Fotsing, Barbu, Beauchant, ABCB4/MDR3 gene mutations and cholangiocarcinomas, J. Hepatol. 57 (2) (2012) 467–468.

[32] P.H. Dixon, M. Sambrotta, J. Chambers, et al., An expanded role for heterozygous mutations of ABCB4, ABCB11, ATP8B1, ABCC2 and TJP2 in intrahepatic cholestasis of pregnancy, Sci. Rep. 7 (2017) 11823, https://doi.org/10.1038/s41598-017-11626-x.